encit 2020

ABCM Associação Brasileira de Engenharia e Ciências Mecânicas

18th Brazilian Congress of Thermal Sciences and Engineering
November 16-20, 2020, (Online)

ENC-2020-0231
MULTI-PARAMETER ESTIMATION IN ACTIVE DESICCANT WHEELS

Nóbrega, C.E.L.
Brum,N.C.L.
Eng. Computação/CEFET-RJ/ Campus Petrópolis, PEM/UFRJ/COPPE
nobrega@pobox.com
nisio@mecanica.coppe.ufrj.br

Abstract. *The quest for low energy demand acclimatization systems has led to the application of active desiccant wheels, as an effective dehumidification tool. It consists of a porous matrix impregnated with a desiccant substrate, which swings between the fresh air stream and a reactivation hot air stream. The dynamic behaviour of desiccant wheels has been simulated by a mathematical model, which has been tested and validated by comparison with experimental data, allowing for the design of increasingly effective units. However, the continuous operation can lead to a deviation of the original design parameters. For instance, fouling can concur to pore blockage, thereby modifying the adsorption capacity in addition to heat and mass transfer coefficients. An inverse problem methodology is proposed to retrieve original design parameters.*

Keywords: *Desiccants, Inverse Problems, Parameter Estimation*

1. INTRODUCTION

Active desiccant wheels can are tailored to continuously dehumidify an air stream, allowing for independent humidity and temperature controlled environments. The hygroscopic mesoporous matrix is alternatively exposed to process air and regeneration streams, in a periodic heat and mass transfer process. Although the design parameters featured in the equations that comprise the mathematical model are set at the design stage, the daily operation can lead to significant variations on these values. For instance, the continuous deposition of particles and oxides can concur to an overall thermal resistance increase. Although external air should be properly filtered, the desiccant layer is unavoidably exposed to fine particles, organic compounds and other contaminants which often deposit in the micro-pores, hindering the adsorptive capacity. The fouling layer modifies the original start up value of the heat transfer coefficient, thereby causing an effectiveness decrease (Nellis, 2019). Moreover, temperature difference between hot and cold hemispheres can result in gasket failure, allowing for air leakage. Moreover, leakage can occur through the seals which keep the streams apart, or through the circumferential gap between the wheel and housing (Beck, 1996). Additionally, excessive regeneration temperature and thermal stress can progressively result in deterioration (Nakabayashi et al., 2011) and desiccant layer deliquescence, with consequent loss of adsorptive capacity (Asim et al., 2019). For instance, silica-gel and alumina have been reported to rapidly deteriorate for higher regeneration temperatures (Belding et al., 2016) and (Oliveira et al., 2019).

Accordingly, the present effort proposes a parameter estimation methodology for heat and desiccant wheels based on transient temperature measurements. The procedure is validated by generating by setting values for the sought parameters, thereby generating an “exact” solution for the direct problem, in which the value of temperature record in three different locations is calculated and stored in arrays. A randomly generated noise of specified standard deviation and Gaussian distribution around zero is then added to each of these array elements, which now bears the characteristic random fluctuation of experimental data. The inverse problem methodology is then applied in trying to estimate the original parameters values which generated the “experimental data” (Orlande and Ozisik, 1999). Fouling growth has been addressed by stochastic (Zubair and Kureshi, 2016) and mechanistic models (Balakrishnan et al., 1992). As for inverse design, a parameter-estimation technique showed to predict the parameters of a fouling correlation within 10% accuracy in for crude oil distillation process (Costa et al., 2013). The conjugate gradient inverse method has been applied to predict the shape of fouling layers in pipe internal walls (Chen et al., 2009). Parameter estimation techniques have been successfully applied to mass transfer problems, such as in column adsorption reactors (Folly et al., 2005) solid-liquid systems (Vasconcelos et al., 2003) and porous slabs (Orlande and Saker., 2004), in addition to thermal resistance evaluation on alloy interfaces (Kanjanakijkasen, 2016).

2. THE DIRECT PROBLEM

Figure (1) describes the computational field, detached from a transversal section of the regenerator. The model is developed under the simplifying assumptions:

1) The thermal capacitance of hot and cold streams is negligible, compared to the matrix thermal capacitance.
2) Thermo physical properties are constant.
3) The flow in the channel is hydro dynamically developed
4) The hot and cold flow rates are balanced.
5) Constant fluid and material temperatures in any cross section of the channel (lumped formulation in the y-direction)
6) The regenerator is perfectly insulated.
7) Convective coefficients are uniformly distributed along the flow.
8) Due to the thickness/length ratio, thermal conductance within the storage material is negligible in the flow direction and finite in the normal direction to it.
9) Temperature and concentration distributions in the direction normal to the flow are taken to be uniform (lumped) within the channel and the solid.
10) The adsorption heat is modeled as a heat source within the flow channel.

Details of the mathematical model development and validation are widely available in the literature, (Nóbrega and Brum, 2009), (Nóbrega and Brum, 2011), (Nóbrega and Brum, 2014) and (Chung and Lee, 2009). In short, energy and mass balances are applied to elementary control volumes enclosing the sorbent layer and the flow channel, resulting in equations (1) to (4), and an algebraic equation (5) which relates the adsorptive capacity as a function of the vapor pressure in the pore vicinity, known as isotherm. Auxiliary psichrometric equations (not presented) allow for relating air relative humidity ϕ_w to the absolute humidity of air in contact with the pores, Y_w^*, and air enthalpy to humidity and temperature

$$\frac{\partial Y^*}{\partial x^*} = \lambda_3 \left(Y_w^* - Y^* \right) \tag{1}$$

$$\frac{\partial W}{\partial t^*} = \lambda_2 \left(Y^* - Y_w^* \right) \tag{2}$$

$$\frac{\partial T_a}{\partial x^*} = T_w - T_a \tag{3}$$

$$\frac{\partial T_w}{\partial t^*} = \left(T_a - T_w \right) + \lambda_1 \left(Y^* - Y_w^* \right) \tag{4}$$

$$\frac{W}{W_{\max}} = \frac{1}{(1 - R + \frac{R}{\phi_w})} \tag{5}$$

$$\lambda_1 = \frac{q}{\left(\frac{\partial h_a}{\partial T_a} \right)} \tag{6}$$

$$\lambda_2 = \frac{C_{wr}}{f \left(\frac{\partial h_a}{\partial T_a} \right)} \tag{7}$$

$$\lambda_3 = \frac{k_y}{h_w}\left(\frac{\partial h_a}{\partial T_a}\right) \tag{8}$$

$$q = h_v\left(1.0 + 0.284e^{-10.28W}\right) \tag{9}$$

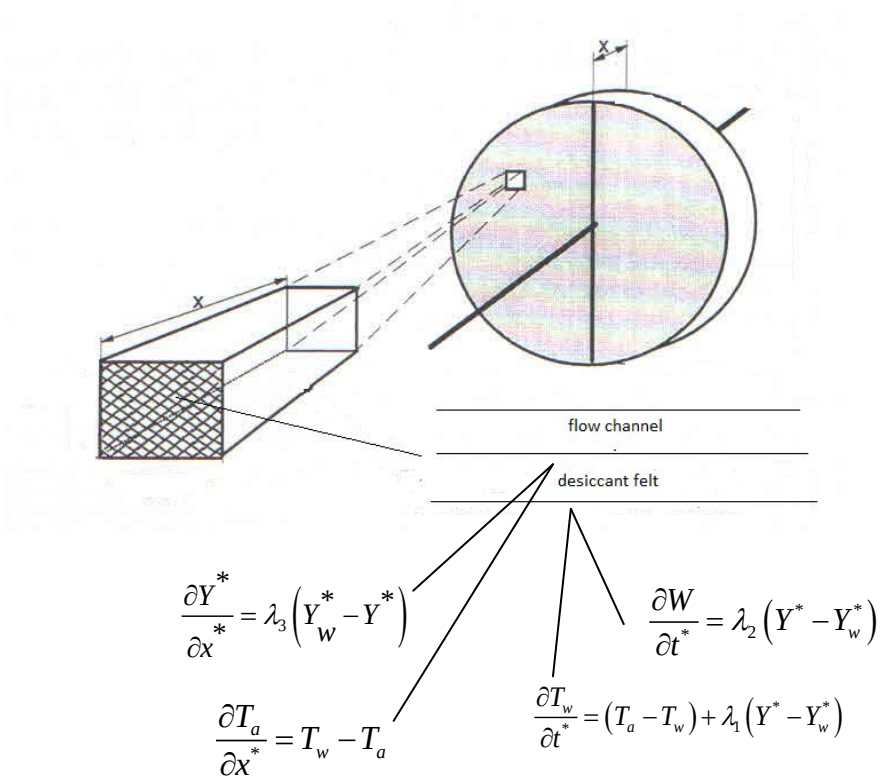

Figure 1: Unitary non-dimensional domain (desiccant felt and flow channel)

In Eqs. (1) through (9), the symbols refer respectively to

C_{wr}	wall specific heat (kJ/kg K)
f	desiccant mass fraction
h	convective heat transfer coefficient (KW/m^2)
h_a	air enthalpy (kJ/kg)
k_y	convective mass transfer coefficient (kg/m^{2}s)
h_v	heat of vaporization (kJ/kg)
q	heat of adsorption (kJ/kg)
R	Separation factor
t^*	time (dimensionless)
T_a	air temperature (°C)
T_w	wall temperature (°C)
Y^*	air absolute humidity (kg/kg air)
Y_w^*	air layer (in pore surface) absolute humidity (kg/kg air)
W	desiccant humidity (kg of moisture/kg of desiccant)
x*	coordinate (dimensionless)

The periodic nature of the problem implies an iterative procedure. Both initial distributions of temperature and humidity within the solid are guessed, and equations (1) to (4) assume the form of tri-diagonal matrices, as a result of the discretization using the finite-volume technique (Majumdar, 2005). Convective terms are represented by an upwind scheme, whereas a fully implicit scheme represents the transient terms. By the end of the cycle, both calculated

temperature and moisture fields are compared to the initially guessed fields, replacing it while convergence is not attained.Since the wheel is to store neither energy nor mass after a complete cycle,

$$\sum \dot{m}_i \, h_i = \sum \dot{m}_o \, \overline{h}_o \tag{10}$$

or else

$$\dot{m}_h \, h_{hi} + \dot{m}_c \, h_{ci} = \dot{m}_h \, \frac{1}{p_h} \int_0^{p_h} h_{ho} \, dt^* + \dot{m}_c \, \frac{1}{p_c} \int_0^{p_c} h_{co} \, dt^* \tag{11}$$

where $\dot{m}$ represents the air mass fluxes, (kg/s), and $P_{h,c}$ stands for the cold and hot periods (s) . The normalized difference between the two sides of equation (14) is defined as the Heat Balance Error (HBE):

$$HBE = \frac{\dot{m}_h \, h_{hi} + \dot{m}_c \, h_{ci} - (\dot{m}_h \, \frac{1}{p_h} \int_0^{p_h} h_{ho} \, dt^* + \dot{m}_c \, \frac{1}{p_c} \int_0^{p_c} h_{co} \, dt^*)}{\dot{m}_h \, h_{hi} + \dot{m}_c \, h_{ci}} \tag{12}$$

The subscripts refer to control volume inlets and outlets,

hi hot inlet
ho hot outlet
ci cold inlet
co cold outlet

Tables (1) and (2) show the temperature T_w and humidity content W distributions for the desiccant layer, for a typical period of revolution. The periodic behaviour can be verified by comparing the first and last columns in both tables. The results were obtained for a grid of 91 points with a non-dimensional time interval δt of 10^{-3}. Convergence was attained after 173 iterations for a HBE lesser than 10^{-4}.

Table 1: Typical temperature distribution through a complete revolution, $T_w(x)$,˚C

0º	45º	90º	135º	180º	225º	270º	315º	360º
69.98	86.78	87.31	87.75	88.11	73.72	70.64	70.28	69.94
67.89	83.87	84.46	84.99	85.47	70.78	68.65	68.26	67.87
66.71	82.23	82.86	83.44	83.98	69.27	67.54	67.12	66.69
62.66	76.77	77.53	78.24	78.93	64.67	63.71	63.18	62.65
59.54	72.69	73.54	74.32	75.08	61.46	60.71	60.12	59.54
57.86	70.52	71.41	72.22	73.01	59.78	59.07	58.46	57.86
52.37	63.58	64.55	65.37	66.20	54.30	53.62	52.99	52.37
46.35	56.11	57.03	57.73	58.46	47.99	47.40	46.86	46.35
39.16	47.91	49.21	50.01	50.71	41.37	40.65	39.90	39.16

Table 2: Typical humidity distribution through a complete revolution, W (x) kg/kg.

0º	45º	90º	135º	180º	225º	270º	315º	360º
0.0418	0.0413	0.0404	0.0396	0.0390	0.0394	0.0401	0.0409	0.0418
0.0471	0.0466	0.0455	0.0445	0.0436	0.0442	0.0451	0.0461	0.0471
0.0583	0.0575	0.0559	0.0544	0.0530	0.0539	0.0553	0.0568	0.0583
0.0745	0.0731	0.0708	0.0686	0.0665	0.0678	0.0700	0.0722	0.0745
0.0992	0.0970	0.0935	0.0902	0.0870	0.0892	0.925	0.0958	0.0992
0.1420	0.1383	0.1328	0.1276	0.1225	0.1263	0.1314	0.1367	0.1420
0.1650	0.1605	0.1540	0.1476	0.1415	0.1462	0.1524	0.1586	0.1650
0.1971	0.1915	0.1835	0.1756	0.1680	0.1739	0.1816	0.1893	0.1971
0.2871	0.2768	0.2642	0.2525	0.2413	0.2523	0.2649	0.2766	0.2871

3. THE INVERSE PROBLEM

The experimental data required by methodology will be obtained by means of a "simulated experiment", described in step 1. The methodology uses the conjugate gradient method, with the objective function (norm) given by the difference between measured and calculated temperatures, which is to be minimum when the latter is evaluated using the correct estimated values for the parameter vector **P**. In short, the estimative of the parameter vector **P** involves the following procedure (Orlande and Ozisik, 1999):

1. Solve the direct problem with known values for the parameter vector $\mathbf{P}^k$ and obtain a solution vector $\mathbf{T}\left(\mathbf{P}^k\right)$, which represents the (calculated) temperature values. Then add a perturbation to each vector element by random values with null average and specified maximum deviation σ, so as to obtain the vector $\mathbf{T}_{meas}$ with known accuracy, which plays the role of an array obtained experimentally. The recorded temperatures are at the wall channel outlet (Sensor A), channel air outlet (sensor B) and wall channel midway, (sensor C). Erase the elements of **P**, which are to be retrieved by the methodology.

2. Set the iteration counter k=1, and solve the direct problem with guessed values for the vector $\mathbf{P}^k$ and obtain a solution vector $\mathbf{T}_{calc}\left(\mathbf{P}^k\right)$, which represents the (calculated) temperature values.

3. Calculate the norm S according to

$$S\left(\mathbf{P}^k\right)=\left[\mathbf{T}_{meas}-\mathbf{T}_{calc}\left(\mathbf{P}^k\right)\right]^T\left[\mathbf{T}_{meas}-\mathbf{T}_{calc}\left(\mathbf{P}^k\right)\right] \tag{13}$$

4. Check for the stopping criterion given by $S\left(\mathbf{P}^k\right)\le\varepsilon$, continue if not attained.
5. Calculate the sensitivity matrix according to

$$\mathbf{J}^k\left(\mathbf{P}\right)=\left[\frac{\partial\mathbf{T}^T\left(\mathbf{P}\right)}{\partial\mathbf{P}}\right]^T \tag{14}$$

Using a central finite-difference scheme to calculate each matrix component

6. Knowing $\mathbf{J}^k, \mathbf{T}_{meas}$ *and* $\mathbf{T}_{calc}\left(\mathbf{P}^k\right)$, compute the gradient direction from

$$\nabla S\left(\mathbf{P}^k\right)=-2\left(\mathbf{J}^k\right)^T\left[\mathbf{T}_{meas}-\mathbf{T}_{calc}\left(\mathbf{P}^k\right)\right] \tag{15}$$

7. Compute the conjugation factor γ from the Polak-Ribiere formula (Beck and Blackweel, 1985)

$$\gamma^k=\frac{\sum_{j=1}^{N}\left[\left[\nabla S\left(\mathbf{P}^k\right)\right]_j\left[\nabla S\left(\mathbf{P}^k\right)-\nabla S\left(\mathbf{P}^{k-1}\right)_j\right]\right]}{\sum_{j=1}^{N}\left[\nabla S\left(\mathbf{P}^{k-1}\right)\right]_j^2} \tag{16}$$

8. Compute the direction of descent $\left(\mathbf{d}^k\right)$ given by

$$\mathbf{d}^k=\nabla S\left(\mathbf{P}^k\right)+\gamma^k\mathbf{d}^{k-1} \tag{17}$$

9. Compute the search step size β from

$$\beta^k=\frac{\left[\mathbf{J}^k\mathbf{d}^k\right]\left[\mathbf{T}_{calc}\left(\mathbf{P}^k\right)-\mathbf{T}_{meas}\right]}{\left[\mathbf{J}^k\mathbf{d}^k\right]^T\left[\mathbf{J}^k\mathbf{d}^k\right]} \tag{18}$$

10. Compute the new parameter vector from

$$\mathbf{P}^{k+1}=\mathbf{P}^k-\beta^k\mathbf{d}^k \tag{19}$$

11. Update iteration counter by replacing k by k+1 and return to step1

4. RESULTS

The simulated experiment was carried out for the four-element parameter array **P** shown in Table 3, with all parameters equal to unity. The initial guess for elements 1 to 4 of the parameter vector $\mathbf{P}^0$ was taken as [0.588; 0.317; 0.612; 0.471]. The methodology was able to retrieve actual parameter values with a lesser than 1% error for a noiseless input, whereas for a ±0.5% noise the errors ranged from 1 to 5%. Even for a ±1.0% noise, results showed to be very accurate. Since the maximum temperature in the problem is 90˚C, a 1% noise corresponds to ±0.9 ˚C, which is achievable by most temperature measurement methods. The greatest error is in the retrieval of parameter λ_2 (element 3 on parameter array **P**). Figures (2) to (4) show the sensitivity coefficients along the cycle for sensors A, B and C. Sensors A and B are on the same longitudinal position, reading temperatures in the desiccant layer and air at the channel outlet, respectively, whereas sensor C reads the temperature at desiccant layer at mid-length. In each case Parameters 1 and 2 (R and λ_1) show to have sensitivity coefficients two orders of magnitude smaller than parameters 3 and 4 (λ_2 and λ_3), which however didn´t prevent their values to be estimated. It can be observed some correlation between parameters 3 and 4 up to the first half of the period. Parameters 1 and 2, conversely, are more clearly independent up to the first half of the period. All calculations were carried out until the residuals between measured and estimated temperatures are of the same magnitude of the noise introduced to generate the measurements array.

Table 3:Exact and Estimated Parameters for Increasing Noise Levels

i	**Parameter Array**	**Exact**	**$\sigma = 0$**	**$\sigma = 0.005T_{meas,\,max}$**	**$\sigma = 0.01T_{meas,\,max}$**
1	R	1.000	1.005	1.036	1.046
2	**λ_1**	1.000	1.000	0.999	1.005
3	**λ_2**	1.000	0.998	1.037	1.144
4	**λ_3**	1.000	1.000	1.001	1.011

The use of additional sensors showed no further improve of convergence. The algorithm also showed to be stable in relation to the random errors introduced in the measurements array. The methodology requires a reasonable computational effort, since the periodic nature of the direct problem requires around 150 iterations to converge. Since the sensitivity coefficients are solved by central difference scheme, (which implies the problem to be solved twice, back and forth), the parameter vector has 4 elements, the measurements array has 20 elements and there are 3 sensors, the direct problem is solved 480 times per iteration of the conjugate gradient scheme. Since the conjugate gradient requires around 50 iterations to converge with the reported initial guess and stopping criteria, the direct problem is solved over 3.6E+6 times. However, since the direct problem consists of 4 tri diagonal matrices of 91 lines each (Eqs (1) to (4) after discretization), which are easily solved by Thomas (TDMA) algorithm, (Majumdar, 2005), the overall computational effort turns out to be feasible on a personal computer. The methodology was also shown to be stable regarding the initial guess for the parameter vector **P**, with successful estimates from a randomly generated elements with uniform distribution between [0,1].

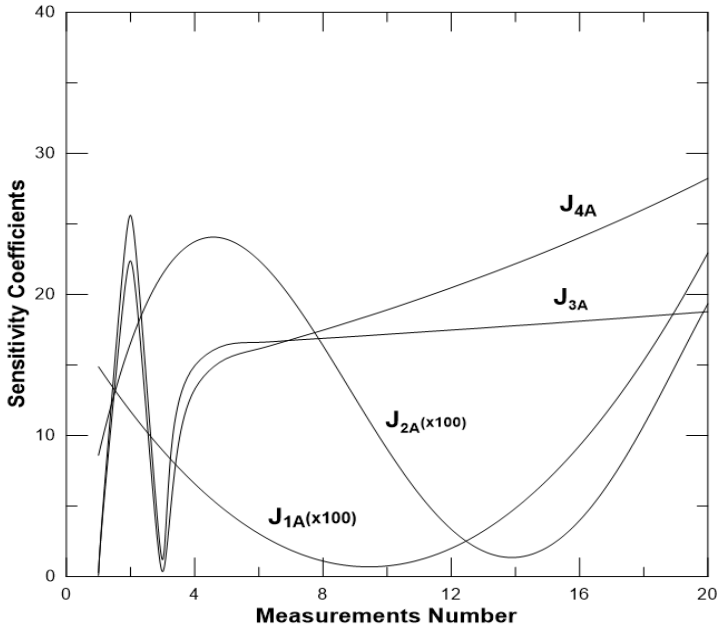

Figure 2: Sensitivity coefficients, sensor A

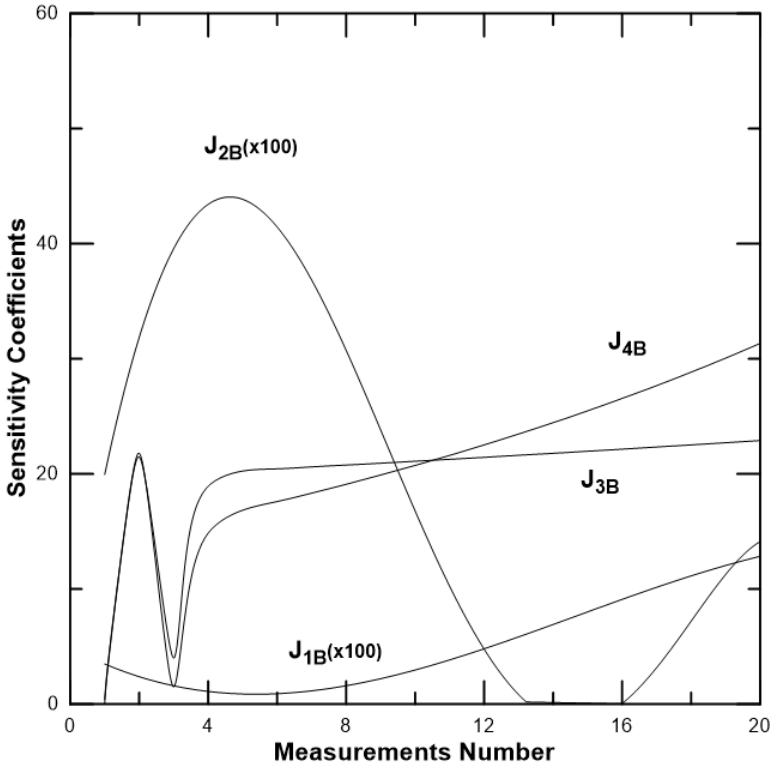

Figure 3: Sensitivity coefficients, sensor B.

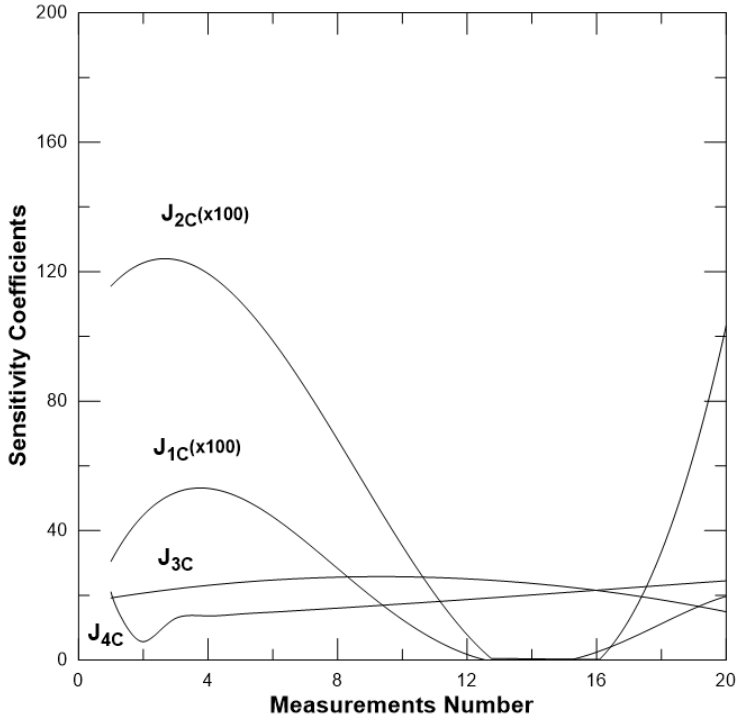

Figure 4 Sensitivity coefficients, sensor C.

5. CONCLUSION

In its continuous operation, desiccant wheels are subjected to a number of factors, such as fouling or gasket leakage, which can lead parameters to deviate from its original design figures. Accordingly, the present paper addresses the estimation of off-design parameters in desiccant wheels. The direct problem was addressed by the finite-volume technique, whereas the minimization was carried out by the conjugate gradient method. The inverse problem methodology was developed and tested, and the conjugate gradient method showed to provide an effective tool for minimizing the difference between calculated and experimental results, obtained by adding randomly generated errors to the exact solution. The iterative nature of the direct problem, in addition to the numerical evaluation of the sensitivity coefficients amounted to a reasonable computational effort. It was shown that the proposed methodology allows for the retrieval of as much as four parameters with the use of three temperature sensors even with a standard deviation of ±0.9 ˚C, which is a reasonable figure even for hand-held sensors. The methodology avoids the use of humidity measurements, which are usually less accurate when compared to temperature measurements, and can be used to maintenance rescheduling, such as matrix cleaning and gasket seal adjusting.

6. REFERENCES

Asim,N., Amin, M.H., Alghoul, M.A., Baidei, M., Mohammad,M., Gasaymesh,S.S., Amin,N., Spoian,K., 2019. “Key factors of desiccant-based cooling systems: Materials”, *Applied Thermal Engineering*, (159) 113946.

Balakrishnan, S., Nagarajan, R., Karthick, K.,1992. “ Mechanistic modelling, numerical simulation and validation of slag-layer growth in a coal-fired boiler”, *Energy*, vol.81, pp.462-470.

Beck S.D., Wilson D.G.,1996. *Gas Turbine Regenerators*. Chapman & Hall, New York.

Beck, J.V., Blackwell B., St Clair,C.R., 1985. *Inverse Heat Conduction*, John Wiley & Sons, New Jersey.

Belding W.A., Delmas, M.P.F., Holeman W.D., 2016.”Desiccant aging and its effects on desiccant cooling system Performance”, *Applied Thermal Engineering* 16 (5), pp. 447-459.

Chen W.L., Yang Y.C., Lee H.L., 2009. “Three-Dimensional pipe fouling layer estimation by using conjugate gradient method” , *Numerical Heat Transfer, Part A*, (55) , pp. 845-865.

Chung JD, Lee, DY. ,2009.” Effect of desiccant isotherm on the performance of desiccant wheel”, *International Journal of Refrigeration,Vol 32,No1*, pp 720-726.

Costa A.L.H., Tavares V.B.G., Borges J.L., Queiroz E.M., Pessoa F.L.P., Liporace F.S., Oliveira, S.G., 2013. “Parameter estimation of fouling Models in crude preheat trains”, *Heat Transfer Engineering*, 34, (8-9), pp. 683-691.

Folly F. M., Silva Neto, A. J. e Santana C. C., 2005. “An inverse mass transfer problem for the characterization of simulated moving beds adsorption columns”, *Proceedings of the 5th International Conference on Inverse Problems in Engineering: Theory and Practice*, Cambridge, UK.

Kanjanakijkasen,W., ”Estimation of spatially varying thermal contact resistance from finite element solutions of boundary inverse heat conduction problems split along material interface”,2016. *Applied Thermal Engineering* 106, pp. 731-742.

Majumdar P. . *Computational Methods for Heat and Mass Transfer*, Taylor & Francis, New York, NY, (2005).

Nakabayashi,S., Nagano K, Nakamura M., Togaua J., Kurokawa A., 2011. “Improvement of water vapor adsorption ability of natural mesoporous materials by impregnating with chloride slats for development of a new desiccant filter”, *Adsorption*, (17), pp.675-686.

Nellis G., Klein S., 2019. *Heat Transfer*, Cambridge University Press, Cambridge, 2019.

Nóbrega C.E., Brum N.C.L ., 2009, "Modeling and simulation of heat and enthalpy recovery wheels", *Energy* (34) , n˚12, pp 2063-2068.

Nóbrega C.E., Brum N.C.L ., 2011, "A graphical procedure for desiccant cooling cycle design", *Energy* (36),n˚3, pp 1564-1570.

Nóbrega C.E.L., Brum N.C.L., 2014. "An Introduction to Solid Desiccant Cooling Technology", in *Desiccant-Assisted Cooling"* edited by C.E.L. Nóbrega and N.C.L. Brum, Springer-Verlag, London.

Oliveira, E.P., Siteven, G.M., Lins, E.F., Vaz, J.R.P., 2019. "Desiccant aging and its effects on desiccant cooling system performance", *Applied Thermal Engineering* (155), pp. 365-372.

Orlande H. R. B. , Saker L. F, 2004. "Simultaneous estimation of spatially-dependent mass and heat transfer coefficients of drying bodies", *Inverse Problems in Science and Engineering* vol. (12), n˚.5, pp. 549-561

Orlande H.R.B., Ozisik N.M., 1999. *Inverse Heat Transfer*, Taylor & Francis, New York, NY.

Patankar S., *Numerical Heat Transfer and Fluid Flow*, Hemisphere Publishing Co., Boston,1980.

Vasconcellos J. F. V., Silva Neto A. J. e Santana, C. C., 2003."An inverse mass transfer problem in solid-liquid adsorption Systems", Inverse *Problems in Engineering*, Vol. (11), No. 5, pp. 391-408.

Zubair S.M., Kureshi B.A.,2016. "The impact of fouling on the performance of a vapour compression refrigerant system with integrated mechanical sub-cooling system", *Applied Energy*, vol. 92 (C), pp. 750-762.

7. RESPONSIBILITY NOTICE

The author(s) is (are) the only responsible for the printed material included in this paper.